

## SUPPORTING INFORMATION

### Local ionic liquid environment at a modified iron porphyrin catalyst enhances electrocatalytic performance of CO<sub>2</sub> to CO reduction in water

Asma Khadhraoui,<sup>a</sup> Philipp Gotico,<sup>b</sup> Bernard Boitrel,<sup>c</sup> Winfried Leibl,<sup>b</sup> Zakaria Halime,<sup>a\*</sup> and Ally Aukauloo<sup>\*a,b</sup>

<sup>a</sup> Laboratoire de Chimie Inorganique (LCI), Institut de Chimie Moléculaire et des Matériaux d'Orsay (ICMMO), Université Paris-Sud, Rue du doyen Georges Poitou, 91405 Orsay, France

<sup>b</sup> Laboratoire des Mécanismes fondamentaux de la Bioénergétique (LMB), Institut de Biologie Intégrative de la Cellule (I2BC), Institut des Sciences du Vivant Frédéric-Joliot, CEA Saclay, 91191 Gif-sur-Yvette, France

<sup>c</sup> Institut des Sciences Chimiques de Rennes, UMR CNRS 6226, Université de Rennes 1, Rennes cedex, France

Correspondence: [zakaria.halime@u-psud.fr](mailto:zakaria.halime@u-psud.fr), [ally.aukauloo@u-psud.fr](mailto:ally.aukauloo@u-psud.fr)

#### Table of Contents

<b>I. Synthesis and characterization of complexes 2 and 3</b> .....	<b>2</b>
General materials and methods .....	2
Synthesis of complex 2 .....	2
Synthesis of complex 3 .....	2
Control experiment.....	3
<b>II. Cyclic Voltammetry and data analysis</b> .....	<b>3</b>
General materials and conditions .....	3
Table S1: redox potentials and catalytic potentials for CO <sub>2</sub> reduction of complexes FeTPP, FeTPPF <sub>8</sub> , FeTPPF <sub>20</sub> and 3 in DMF/ H <sub>2</sub> O 9:1 and 3 in H <sub>2</sub> O. ....	3
Figure S1.....	4
Figure S2.....	4
Foot-of-the-wave analysis for Tafel plots .....	5
<b>III. Bulk electrolysis and products characterization</b> .....	<b>6</b>
Figure S3.....	6
Figure S4.....	7
<b>IV. UV-visible and mass spectra of complexes 2 and 3</b> .....	<b>9</b>
Figure S5.....	9
Figure S6.....	9
Figure S7:.....	10
Figure S8:.....	10
Figure S9:.....	11
<b>V. References</b> .....	<b>11</b>

## I. Synthesis and characterization of complexes **2** and **3**

**General materials and methods:** Dimethylformamide (DMF, Aldrich 99.9%), Tetrahydrofuran (THF, Aldrich 99.8%), tetra-n-butyl ammonium hexafluorophosphate ( $[\text{Bu}_4\text{N}]\text{PF}_6$ , Aldrich 99%) were used as received. All other chemical reagents used in the synthetic route were obtained from commercial sources as guaranteed-grade reagents and used without further purification. Water was Milli-Q filtered (18.2  $\text{M}\Omega\cdot\text{cm}$  at 25 °C) and the pH was adjusted to 7.0 using sodium hydroxide solution. Porphyrins TPP and  $\text{TPPF}_{20}$  were purchased from PorphyChem. The synthesis of  $\text{TPPF}_8$  as well as iron complexes of the three reference porphyrins were prepared following previously reported procedures.<sup>1</sup> The electrospray ionization mass spectrometry (ESI-HRMS) experiments were performed on TSQ (Thermo Scientific, 2009) with an ESI<sup>+</sup> method. UV-visible absorption spectroscopy measurements were performed in solution using 1 cm quartz cuvettes in a Varian Cary 5000 UV-vis-NIR spectrophotometer.

**Synthesis of complex 2:** Porphyrin **1** (500 mg, 0.389 mol) was dissolved in 10 mL of Ar degassed THF then 2,6-lutidine (0.9 mL, 7.781 mol) and  $\text{FeCl}_2$  (345 mg, 2.723 mol) were added to the reaction mixture. After an overnight stirring at room temperature, the solvent was evaporated and the crude material was dissolved in 100 mL of  $\text{CHCl}_3$  then extracted with 100 mL of 0.25 M solution of HCl. The organic phase was filtered through a small plug of silica gel then the solvent was evaporated to give complex **2** as a dark purple solid (470 mg, yield = 88 %).

UV-vis (MeOH):  $\lambda_{\text{max}}/\text{nm}$  ( $10^{-3}\epsilon$ ,  $\text{L}\cdot\text{mol}^{-1}\cdot\text{cm}^{-1}$ ): 341 (29.8), 419 (95.9), 593 (6.4), 656 (3.5).

ESI-HRMS: calculated  $m/z = 1336.2270$   $[\text{M}]^+$  for  $\text{C}_{76}\text{H}_{52}\text{Cl}_4\text{FeN}_8\text{O}_4$ , found 1336.2213.

**Synthesis of complex 3:** Complex **2** (100 mg, 73  $\mu\text{mol}$ ) was dissolved in 5 mL of dry DMF under Ar atmosphere, then 1-methylimidazol was added (23  $\mu\text{L}$ , 291  $\mu\text{mol}$ ) to the reaction mixture at room temperature. After 24 hours stirring at 70° C, the reaction mixture was brought to room temperature then approximately 200 mL of diethylether were added. The obtained purple precipitate was filtered and washed with 2 x 50 mL of diethylether to give iron porphyrin **3** (114 mg, yield = 92 %).

UV-vis (MeOH):  $\lambda_{\text{max}}/\text{nm}$  ( $10^{-3}\epsilon$ ,  $\text{L}\cdot\text{mol}^{-1}\cdot\text{cm}^{-1}$ ): 344 (29.4), 421 (102.8), 594 (5.4), 640 (3.1).

ESI-HRMS: calculated  $m/z = 381.1370$   $[\text{M}]^{4+}$  for  $\text{C}_{92}\text{H}_{76}\text{FeN}_{16}\text{O}_4$ , found 381.1392.

ESI-HRMS: calculated  $m/z = 305.1101$   $[M]^{5+}$  for  $C_{92}H_{76}FeN_{16}O_4$ , found 305.1118.

**Control experiment:** The  $\alpha$ -4 geometry (the four arms in the same side with regard to the porphyrin plan) of porphyrin **1** is maintained at room temperature due to the blocked rotation of the aryl groups on the *meso* positions of the macrocycle. At higher temperature, this rotation become possible and can induce the formation of a mixture of four possible atropoisomers ( $\alpha$ -4,  $\alpha\beta\alpha\beta$ ,  $\alpha\alpha\beta\beta$  and  $\alpha\beta\beta\beta$ ). To confirm the retention of the  $\alpha$ -4 geometry during the synthesis of complex **3**, we performed a control experiment using porphyrin **1**. In this experiment, a solution of **1** in DMF was heated at 70° C for more than 24 hours then TLC and  $H^1$  NMR monitoring of this solution showed no modification of the porphyrin geometry.

## II. Cyclic Voltammetry and data analysis

**General materials and conditions:** Cyclic voltammetry measurements were performed in an electrochemical cell composed of a glassy carbon (3 mm diameter) working electrode, a platinum wire as a counter electrode and an aqueous SCE electrode as the reference electrode. All experiments were carried out under argon or carbon dioxide atmosphere at 25 °C. DMF/water 9:1 mixture or pure water were used as solvent and solutions of catalysts were prepared at a concentration 1 or 0.5 mM. Tertbutylammonium hexafluorophosphate ( $NBu_4PF_6$ ) or potassium chloride (KCl) were used respectively in DMF:water and in water as supporting electrolyte at a concentration of 0.1 M. The solutions were all purged with inert argon gas. AUTOLAB PGSTAT320 was utilized to control the applied voltages and to measure resulting current and the scan rate was chosen at 100 mV/s. Ferrocene was used as a reference for standard comparison in all experiments and then potentials were converted to NHE. Ohmic drop was compensated using the positive feedback compensation implemented in the instrument.

Table S1: redox potentials and catalytic potentials (in V vs NHE) for  $CO_2$  reduction of complexes FeTPP, FeTPPF<sub>8</sub>, FeTPPF<sub>20</sub> and **3** in DMF/ H<sub>2</sub>O 9:1 and **3** in H<sub>2</sub>O.

	$E (Fe^{III}/Fe^{II})$	$E (Fe^{II}/Fe^I)$	$E (Fe^I/Fe^0)$	$E^0_{cat}$
FeTPP	0.091	-0.857	-1.460	-1.430
FeTPPF <sub>8</sub>	0.191	-0.725	-1.329	-1.270
FeTPPF <sub>20</sub>	0.252	-0.635	-1.138	-1.081
<b>3</b>	0.103	-0.733	-1.045	-1.056
<b>3</b> in H <sub>2</sub> O	-0.001	-0.746	-1.028	-1.018

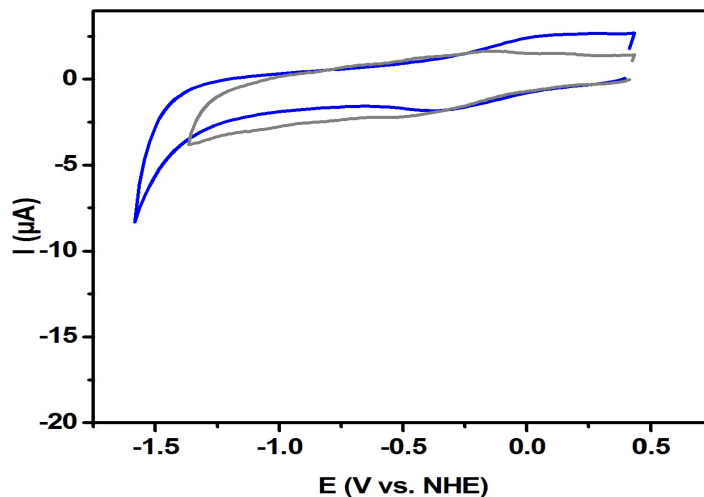


Figure S1: CV of 4.0 mM solution of 1-benzyl-3-methylimidazolium chloride in DMF/H<sub>2</sub>O 9:1 containing 0.1 M of tetra-*N*-butylammonium hexafluorophosphate (TBAPF<sub>6</sub>) at 25°C under argon (gray) and under CO<sub>2</sub> atmosphere (blue).

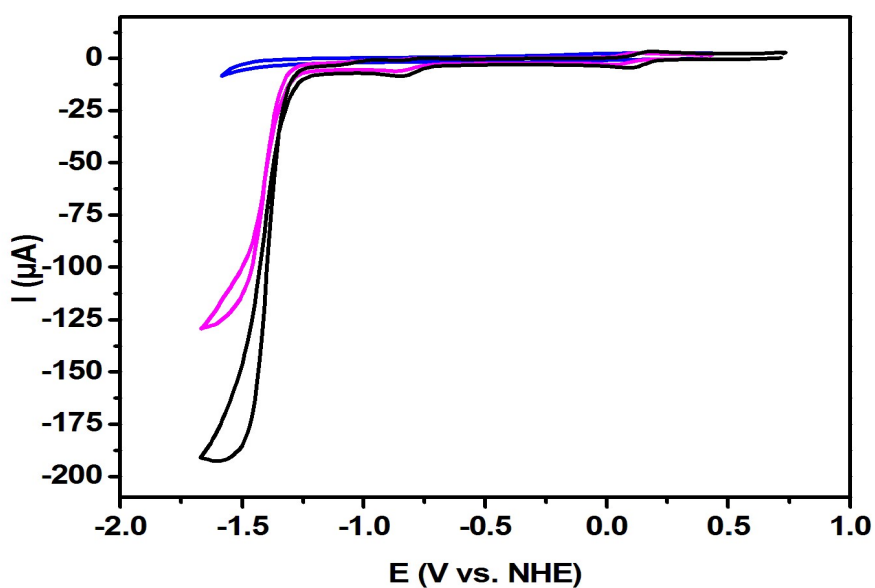


Figure S2: CV of 1.0 mM solution of FeTPP in DMF/H<sub>2</sub>O 9:1 containing 0.1 M of tetra-*N*-butylammonium hexafluorophosphate (TBAPF<sub>6</sub>) at 25°C under CO<sub>2</sub> atmosphere (black), CV of 4 mM solution of 1-benzyl-3-methylimidazolium chloride under similar conditions in absence (blue) and in presence of 1 mM of FeTPP (magenta).

## Foot-of-the-wave analysis for Tafel plots

For fast catalytic process, the foot-of-the-wave analysis of the CVs has been performed as a quick estimation of the catalysis rate constant,  $k_{cat}$  and TOF of the catalytic reaction without contribution from side phenomena such as substrate consumption, catalyst deactivation, and/or product inhibition. The analysis is based on the linear correlation between  $i/i_p^0$  and  $1/\{1+\exp[F/RT(E - E_{cat}^0)]\}$  where:

$i$ : catalytic current in the presence of  $CO_2$

$i_p^0$ : peak current in the absence of  $CO_2$  which was normalized to the second reduction peak current  $i$  of the reversible redox couple under Argon

$F$ : faraday constant

$R$ : gas constant

$T$ : absolute temperature

Plotting  $i/i_p^0$  vs.  $1/\{1+\exp[F/RT(E - E_{cat}^0)]\}$  gives rise to a straight line with a slope =  $2.24(RT/Fv)^{1/2}(k_{cat})^{1/2}$  where  $v$  is the scan rate in  $V s^{-1}$ .

$$\frac{i}{i_p^0} = \frac{2.24 \sqrt{\frac{RT}{Fv}} k_{cat}}{1 + \exp\left[\frac{F}{RT}(E - E_{cat}^0)\right]}$$

$$TOF = \frac{k_{cat}}{1 + \exp\left[\frac{F}{RT}(E - E_{cat}^0)\right]}$$

$$\log TOF = \log k_{cat} - \frac{F}{RT} \ln 10 (E_{CO_2/CO}^0 - E_{cat}^0) + F\eta RT \ln 10$$

$$TOF_{max} = k_{cat}$$

$$\eta = E - E_{CO_2/CO}^0 \quad E_{CO_2/CO}^0 = -0.69 V \text{ vs. NHE in DMF}$$

Then to trace the tafel plot, which is the plot of  $\log TOF$  vs.  $\eta$ , we need the value of  $TOF_0$  which can be determined from the expression below:

$$TOF_0 = \frac{k_{cat}}{1 + \exp\left[\frac{F}{RT}(E_{CO_2/CO}^0 - E_{cat}^0)\right]}$$

$$\log TOF_0 = \log k_{cat} - \frac{F}{RT} \ln 10 (E_{CO_2/CO}^0 - E_{cat}^0)$$

### III. Bulk electrolysis and products characterization

Bulk electrolysis was performed in a CO<sub>2</sub>-saturated water containing 0.1 M KCl as supporting electrolyte at pH = 6.3. A gas-tight two-compartment cell was used for this experiment, each cell having a volume of 43 mL. The first compartment was filled with 20 mL water containing KCl and 0.5 mM catalyst and the working electrode (glassy carbon rod, effective surface area of 1.41 cm<sup>2</sup>) and reference electrode (Ag/AgCl), while the second compartment was filled with 20 mL water containing KCl and contains the counter electrode (10 cm x 3 cm titanium grid with nominal space of 0.19 mm and wire diameter of 0.23 mm). After the electrolysis, the measured pH was 6.4.

Products analysis during the chronoamperometric experiment was performed by withdrawing 50  $\mu$ L gas aliquots from the headspace of the first compartment cell with a gas-tight syringe and injected into a gas chromatography (GC - TraceGC Ultra, ThermoScientific) equipped with a 30 m molecular sieve porous layer open tubular (PLOT) column having an internal diameter of 0.53 mm, helium carrier gas, and a thermal conductivity detector (TCD). Peak separation between H<sub>2</sub>, CO, and CO<sub>2</sub> were achieved by programming the oven temperature from an initial 40 °C for 2 min, ramped by 50 °C/min until a final temperature of 250 °C held for 2 min. H<sub>2</sub> was detected at 2.16 min, CO was detected at 3.13 min, and CO<sub>2</sub> was detected at 6.10 min. A splitless injector line was utilized to maximize the injection volume and become sensitive to possible trace amounts. A calibration curve relating peak area and concentration of CO (or H<sub>2</sub>) was established by injecting known amounts of pure CO (or H<sub>2</sub>) into the experimental set-up (electrolysis cell) and after 10 min equilibration time, 50  $\mu$ L gas aliquots were drawn from the headspace and injected into the GC. This calibration method accounts for the headspace volume of the set-up and any CO dissolved in the solution and as such, it can be used to determine actual amounts of CO (or H<sub>2</sub>) produced.

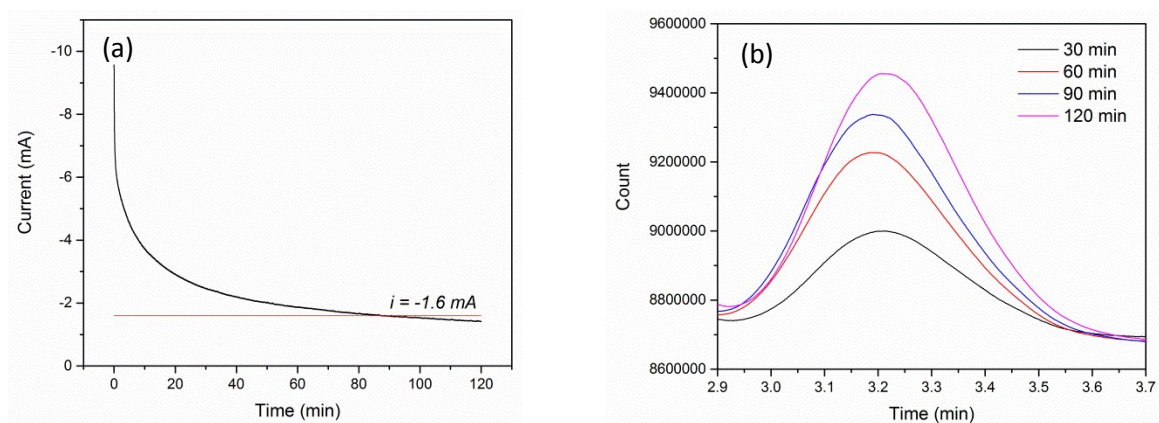


Figure S3: a) Electrolysis current as a function of time for catalyst **3** in a CO<sub>2</sub>-saturated water with 0.1M KCl at  $E_{\text{electrolysis}} = -0.948$  V vs NHE, b) evolution of the produced CO as detected by gas chromatography (in all measurements H<sub>2</sub> gas concentration was less than the limit of detection).

Faradic efficiency (FE) for the 2-electron reduction of CO<sub>2</sub> to CO was calculated using the following:

$$FE = \frac{Q_{exp}}{Q_{theo}} = \frac{2 * F * mol\ CO}{Q_{theo}}$$

where  $F = 96485\text{ C mol}^{-1}$ ,  $mol\ CO$  is the amount of CO detected by GC and  $Q_{theo}$  is the total charge passed, calculated by integrating the current vs. time curve.

The diffusion coefficient of catalyst **3** was determined by plotting peak current as a function of square root of scan rate, following Randles-Sevcik equation:

$$i_p = 0.4463nFAC\left(\frac{nFvD}{RT}\right)^{1/2}$$

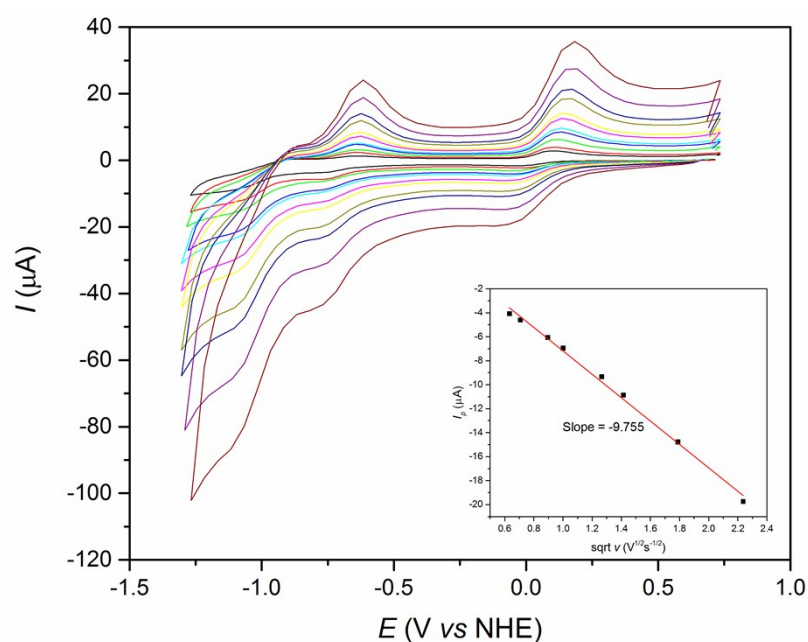


Figure S4: CV's of catalyst **3** (1 mM) at different scan rates in water containing 0.1 M KCl under Ar. Inset shows the diffusion current peak (first reduction peak) as a function of square root of scan rate.

The following parameters were used:  $n$  (electron transferred) = 1,  $F = 96485\text{ C mol}^{-1}$ ,  $R = 8.314\text{ J K}^{-1}\text{ mol}^{-1}$ ,  $T = 298\text{ K}$ ,  $A = 0.07065\text{ cm}^2$  (glassy carbon electrode with diameter of 3 mm),  $C = 1 \times 10^{-6}\text{ mol cm}^{-3}$ . The calculated diffusion coefficient of catalyst **3** in water (0.1 M KCl) is  $2.64 \times 10^{-7}\text{ cm}^2\text{ s}^{-1}$ .

The electrolysis is described by the equation<sup>2-4</sup>:

$$\frac{i}{FA} = \frac{C_{cat}^0 \sqrt{2k_{cat}D_{cat}}}{1 + \exp\left[\frac{F}{RT}(E_{electrolysis} - E_{1/2})\right]}$$

$$k_{cat} = \frac{i^2 \left[1 + \exp\left[\frac{F}{RT}(E_{electrolysis} - E_{1/2})\right]\right]^2}{2F^2 A^2 C_{cat}^0{}^2 D_{cat}} = 2.44 \times 10^5 \text{ s}^{-1}$$

Calculations were made from  $i = -1.5$  mA (taking into account 91% FE for CO production) and the following parameters:  $A$  (electrode surface) =  $1.41 \text{ cm}^2$ ,  $C_{cat}^0$  (catalyst concentration) =  $5 \times 10^{-7} \text{ mol cm}^{-3}$ ,  $D_{cat}$  (catalyst diffusion coefficient) =  $2.64 \times 10^{-7} \text{ cm}^2 \text{ s}^{-1}$ ,  $E_{electrolysis} = -0.948 \text{ V vs NHE}$ ,  $E_{1/2} = -1.018 \text{ V vs NHE}$ ,  $F = 96485 \text{ C mol}^{-1}$ ,  $R = 8.314 \text{ J K}^{-1} \text{ mol}^{-1}$ ,  $T = 298 \text{ K}$ , and  $t$  (electrolysis time) =  $7200 \text{ s}$ . The turnover frequency (TOF) and turnover number (TON) was then calculated using:

$$TOF = \frac{k_{cat}}{1 + \exp\left[\frac{F}{RT}(E_{electrolysis} - E_{1/2})\right]} = 14986 \text{ s}^{-1}$$

$$TON = TOF \times t = 1.08 \times 10^8$$



#### IV. UV-visible and mass spectra of complexes **2** and **3**

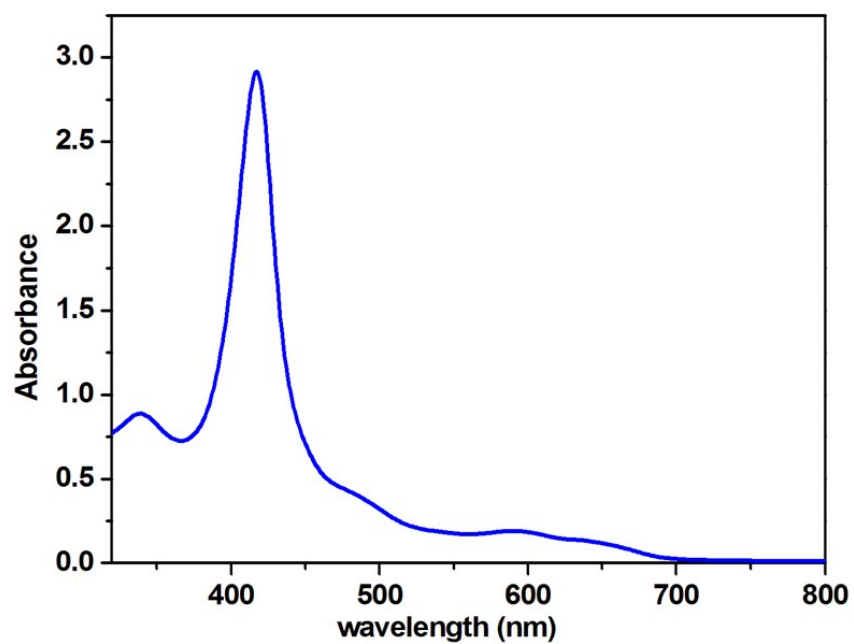


Figure S5: UV-vis spectrum of compound **2** ( $3.0 \times 10^{-5}$  mol/L) in methanol at 25°C.

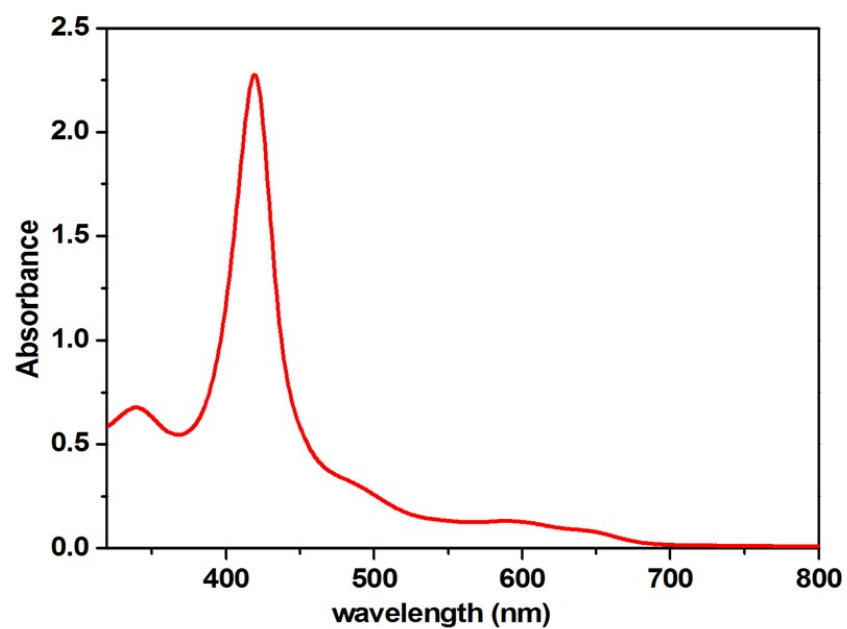


Figure S6: UV-vis spectrum of compound **3** ( $2.4 \times 10^{-5}$  mol/L) in methanol at 25°C.

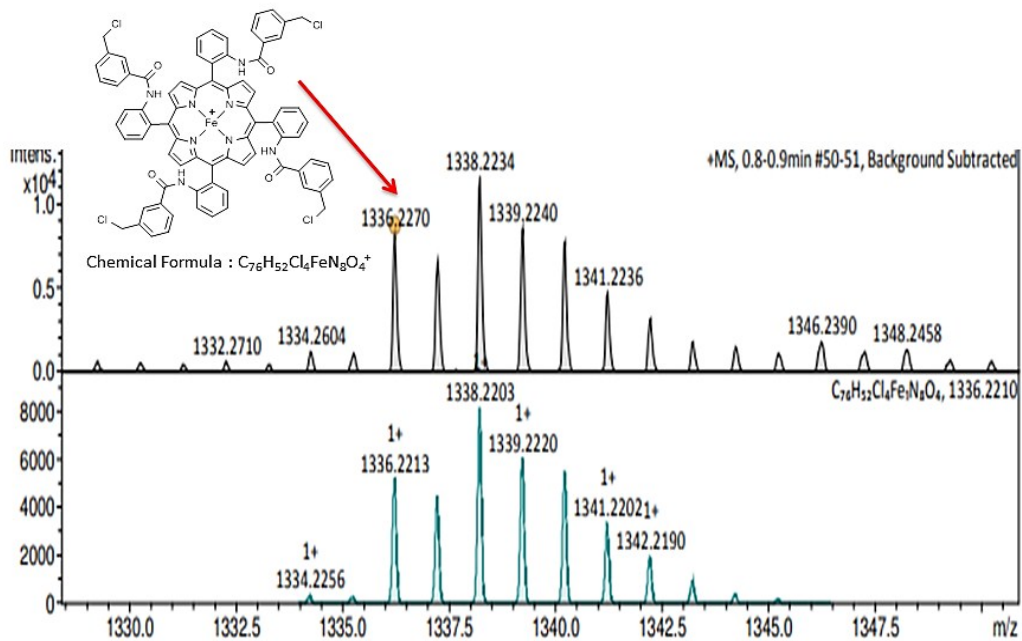


Figure S7: ESI-HRMS spectra of compound  $[2]^+$  (Top) and spectra simulation of compound  $[2]^+$  (bottom).

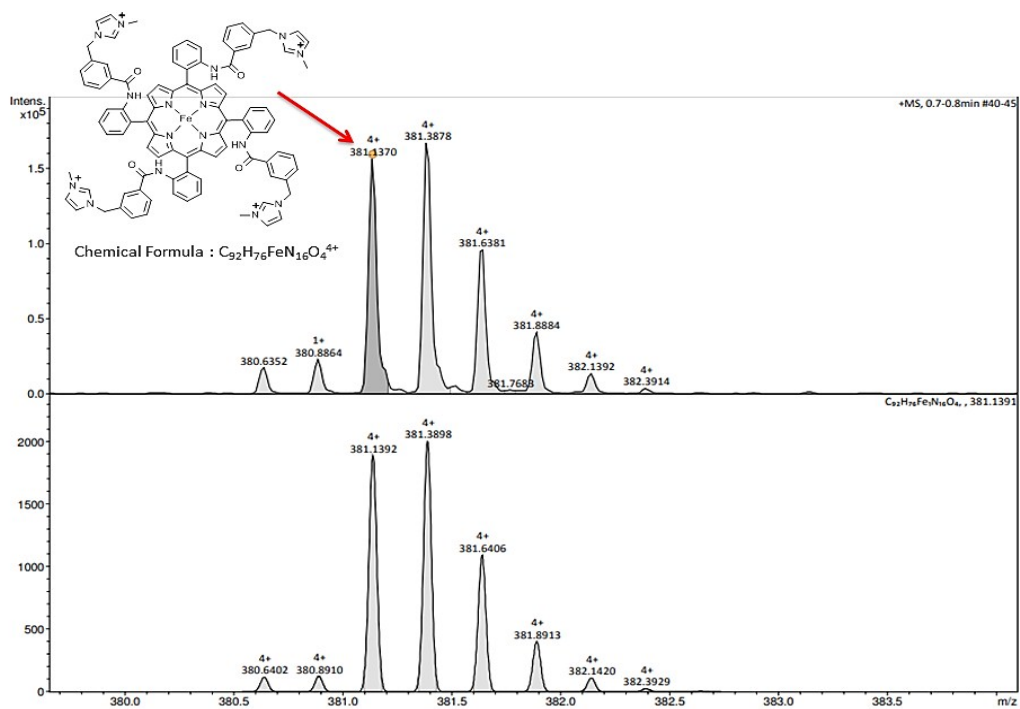


Figure S8: ESI-HRMS spectra of compound  $[3]^{4+}$  (top) and spectra simulation of compound  $[3]^{4+}$  (bottom).

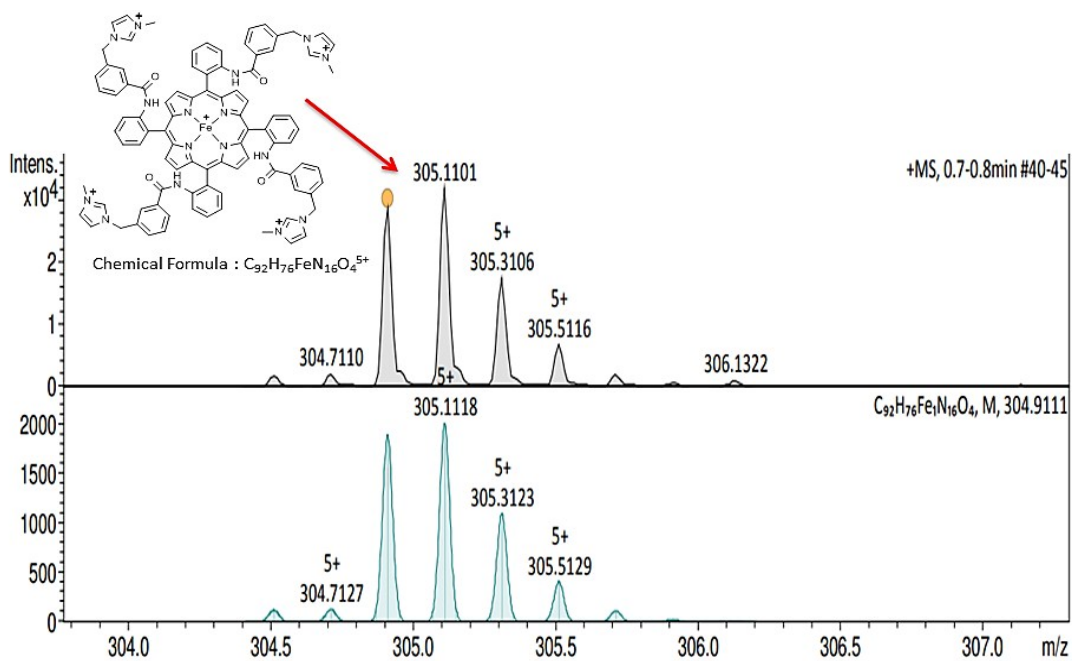


Figure S9: ESI-HRMS spectra of compound **[3]**<sup>5+</sup> (top) and spectra simulation of compound **[3]**<sup>5+</sup> (bottom).

## V. References

1. K. D. Karlin, A. Nanthakumar, S. Fox, N. N. Murthy, N. Ravi, B. H. Huynh, R. D. Orosz and E. P. Day, *Journal of the American Chemical Society*, 1994, **116**, 4753-4763.
2. C. Costentin, S. Drouet, M. Robert and J.-M. Savéant, *J. Am. Chem. Soc.*, 2012, **134**, 11235–11242.
3. C. Costentin, M. Robert and J.-M. Savéant, *Accounts of Chemical Research*, 2015, **48**, 2996–3006.
4. L. Chen, Z. Guo, X.-G. Wei, C. Gallenkamp, J. Bonin, E. Anxolabéhère-Mallart, K.-C. Lau, T.-C. Lau and M. Robert, *J. Am. Chem. Soc.*, 2015, **137**, 10918–10921.